Deconvolution Approach to Multi-compartmental Modeling: Characterizing Intra-Renal Transport of Gadolinium Contrast

J. L. Zhang[1], L. Bokacheva[1], H. Rusinek[1], Q. Chen[1], T. Song[1], N. Oesingmann[2], and V. S. Lee[1]

[1]Department of Radiology, New York University, New York, NY, United States, [2]Siemens Medical Solutions, Malvern, PA, United States

Introduction

Dynamic contrast-enhanced MRI is developing into a valuable imaging technique for non-invasive assessment of renal function. High-resolution MR images allow discrimination of renal cortex, medulla and collecting system. Functional analysis of the intra-renal transport of gadolinium (Gd) contrast between compartments of the vascular-nephron system can be performed using deconvolution to obtain impulse residual functions (IRF). To overcome the inherent ill-conditioned nature of deconvolution process, we derived an explicit multi-exponential form of the IRF based on the tracer kinetics described by a multi-compartmental model (Fig. 1) [1-4]. We demonstrate that incorporating such smooth constraints into deconvolution enables reliable estimation of renal functional parameters such as single-kidney glomerular filtration rate (SK-GFR), and that establishing one set of separable parameters potentially accelerates curve-fitting process.

Theory

In a 4-compartment model, the renal cortex (Cx) consists of vascular (A), proximal tubule (P) and distal tubule (D) compartments (Eq. (1a)), while the renal medulla (Med) consists of vascular (A) and loops of Henle (L) compartments (Eq. (1b)) [2]. Compartment A is distributed in both renal cortex and medulla, with volume $V_{A,Cx}$ and $V_{A,Med}$, respectively. The compartmental Gd concentrations ([A], [P], [L] and [D]) obey linear differential equations (DEs) based on conservation of mass. In implementation, the parameters in the DEs are adjusted to fit the combined [Cx] and [Med] curves in Eq.1 to measured Gd concentration-time curves for each region.

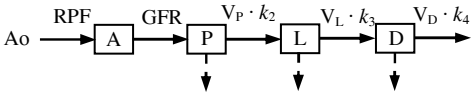

Fig. 1. Four-compartment renal model. RPF: renal plasma flow; GFR: glomerular filtration rate; V_P, V_L and V_D are the compartmental volumes, and k_2, k_3 and k_4 are the regional flow rates in proximal, loop, and distal segments. Solid arrows denote flows with tracer, while dash arrows denote water reabsorption.

$$\begin{cases} [Cx] = \dfrac{V_{A,Cx}}{V_{Cx}}[A] + \dfrac{V_P}{V_{Cx}}[P] + \dfrac{V_D}{V_{Cx}}[D] & (1a) \\ [Med] = \dfrac{V_{A,Med}}{V_{Med}}[A] + \dfrac{V_L}{V_{Med}}[L] & (1b) \end{cases}$$

IRFs for the intra-renal compartments were obtained by solving the 4-compartment DEs with unit-impulse [Ao] (Eq. (2)). IRFs of [A], [P], [L] and [D] consist of 1, 2, 3 and 4 exponential functions, respectively, and incorporate a time delay (TD) for every IRF. Water-reabsorption fraction (f_P, f_L and f_D) and the corresponding compartmental volumes combine into one parameter (regional flow rate k), indicating the inseparability of these 2 types of parameters.

$$\begin{cases} [A](t) = \dfrac{k_1}{1-Hct} e^{-k_1 t} \quad (2a) \qquad [P](t) = \dfrac{GFR\,k_1}{V_P(1-Hct)(k_2-k_1)}\left[e^{-k_1 t} - e^{-k_2 t}\right] (2b) \\ [L](t) = \dfrac{GFR\,k_1 k_2}{V_L(1-Hct)d_4}\left[(k_3-k_2)e^{-k_1 t} - (k_3-k_1)e^{-k_2 t} + (k_2-k_1)e^{-k_3 t}\right] \quad (2c) \\ [D](t) = \dfrac{GFR\,k_1 k_2 k_3}{V_D(1-Hct)d_0}\left[d_1 e^{-k_1 t} - d_2 e^{-k_2 t} + d_3 e^{-k_3 t} - d_4 e^{-k_4 t}\right] \quad (2d) \end{cases}$$

where

$$k_1 = RPF/(V_{A,Cx}+V_{A,Med}) \qquad k_2 = GFR(1-f_P)/V_P$$
$$k_3 = GFR(1-f_P-f_L)/V_L \qquad k_4 = GFR(1-f_P-f_L-f_D)/V_D$$
$$d_0 = (k_2-k_1)(k_3-k_1)(k_4-k_1)(k_3-k_2)(k_4-k_2)(k_4-k_3)$$
$$d_1 = (k_3-k_2)(k_4-k_2)(k_4-k_3) \qquad d_2 = (k_3-k_1)(k_4-k_1)(k_4-k_3)$$
$$d_3 = (k_2-k_1)(k_4-k_1)(k_4-k_2) \qquad d_4 = (k_2-k_1)(k_3-k_2)(k_3-k_1)$$

Patient Study

Nine patients with suspected renovascular disease underwent DCE-MRI at 1.5 T system (Avanto, Siemens) using a coronal 3D FLASH (TR/TE/flip angle=2.84/1.05/12°, 1.7x1.7x2.5 mm^3 voxel, 3s acquisition) after a 4 ml bolus of Gd-DTPA and 20 ml saline flush both at 2 ml/s. Following image registration and segmentation [5] and conversion of signal intensity to Gd concentration [6], model parameters were adjusted by fitting convolution of measured [Ao] and the IRF to their respective measured data, [Cx] and [Med] using Levenberg-Marquardt algorithm. [Cx] data of 0~300s and [Med] of 0~90s were used for fitting. For every patient, ^{99m}Tc-DTPA renal scintigraphy was done in the same morning as MRI. Total GFR was estimated by plasma clearance method, and was split into left and right SK-GFR according to renal uptake at 2-3 min. One kidney was excluded due to presence of multiple cysts.

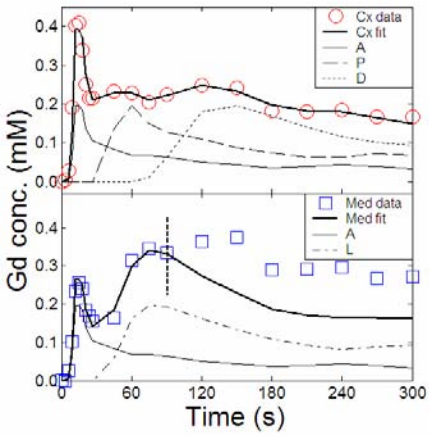

Fig. 2 Fitting of cortical and medullary concentration data, together with the compartmental concentration curves (scaled to same height).

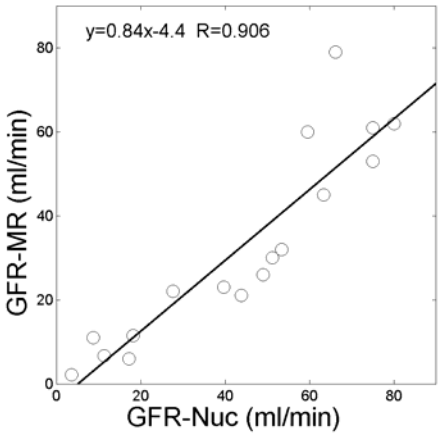

Fig. 3 GFR correlation between MR and nuclear medicine. Regression line: y=0.84x-4.4. Correlation coefficient: R=0.906.

Results and Discussion

Fig. 2 shows an example of [Cx] and [Med] fitting, together with scaled compartmental concentration curves derived from IRFs. The A-peak fits the initial vascular peak in both the [Cx] and [Med] data. P and D define the two broader peaks in the [Cx] with TD of 25s and 64s respectively, while the L defines the initial upslope of medullary peak of TD = 31s, intermediate between P and D. The later part (>90s) of the medullary peak likely reflects collecting duct contributions which are not included in this model. The overall root-mean-square error for fits range from 0.010 to 0.029 mM (0.018±0.005 mM). SK-GFR estimates by the proposed method correlate well with those from nuclear medicine (R=0.906), across a wide range, despite a slight bias (Fig. 3, regression line: y=0.84x-4.4). Deconvolution implementation provides a clear indication of separable model compartments and produces excellent fits to the measured data. The proposed 4-compartmental model has the potential of extracting accurate and detailed functional information about the kidney.

Reference

[1] Buckley D et al. J Magn Reson Imaging 2006;24:1117-1123.
[2] Lee VS et al. In: Proc Intl Soc Magn Reson Med 2003;11.
[3] Annet L et al. J Magn Reson Imaging 2004;20:843-849.
[4] Fine DR et al. Physiol Meas 1994;15:407-428.
[5] Huang AJ et al. In: Proc Intl Soc Magn Reson Med 2003;11.
[6] Bokacheva L et al. Magn Reson Med 2006;55:1186-1190.